

Stem Cell Dynamics in an Experimental Model of Stroke

Min-Cheol Lee, Chun-Yan Jin, Hyung-Seok Kim, Jae-Hyu Kim¹, Myeong-Kyu Kim²,
Hyung-Ihl Kim³, Young-Jin Lee⁴, Young-Jun Son⁴, Young-Ok Kim⁴ and Young-Jong Woo^{4*}

Departments of Pathology, ¹Neurosurgery, ²Neurology, Chonnam National University Medical School, ³Department of Medical Science Engineering, Gwangju Institute of Science and Technology, ⁴Department of Pediatrics, Chonnam National University Medical School, Gwangju, Korea

We investigated the migration of endogenous neural stem cells (NSCs) toward an infarct lesion in a photo-thrombotic stroke model. The lesions produced by using rose bengal dye (20 mg/kg) with cold light in the motor cortex of Sprague-Dawley rats were also evaluated with sequential magnetic resonance imaging (MRI) from 30 minutes through 8 weeks. Migration of NSCs was identified by immunohistochemistry for nestin monoclonal antibody in the lesion cortex, subventricular zone (SVZ), and corpus callosum (CC). The contrast to noncontrast ratio (CNR) on MRI was greatest at 12 hours in DWI and decreased over time. By contrast, T1-weighted and T2-weighted images showed a constant CNR from the beginning through 8 weeks. MRI of the lesional cortex correlated with histopathologic findings, which could be divided into three stages: acute (edema and necrosis) within 24 hours, subacute (acute and chronic inflammatory cell infiltration) at 2 to 7 days, and chronic (gliofibrosis) at 2 to 4 weeks. The volume of the infarct was significantly reduced by reparative gliofibrosis. The number of nestin⁺ NSCs in the contralateral SVZ was similar to that of the ipsilateral SVZ in each group. However, the number of nestin⁺ NSCs in the ipsilateral cortex and CC increased at 12 hours to 3 days compared with the contralateral side ($p < 0.01$) and was reduced significantly by 7 days ($p < 0.01$). Active emigration of internal NSCs from the SVZ toward the infarct lesion may also contribute to decreased volume of the infarct lesion, but the self-repair mechanism by endogenous NSCs is insufficient to treat stroke causing extensive neuronal death. Further studies should be focused on amplification technologies of NSCs to enhance the collection of endogenous or transplanted NSCs for the treatment of stroke.

Key Words: Stroke; MRI; Neural stem cell; Dynamics

This is an Open Access article distributed under the terms of the Creative Commons Attribution Non-Commercial License (<http://creativecommons.org/licenses/by-nc/3.0>) which permits unrestricted non-commercial use, distribution, and reproduction in any medium, provided the original work is properly cited.

INTRODUCTION

Transient and permanent occlusion of the middle cerebral artery (MCA) or thermocoagulation of vessels in the pia mater has been widely used to induce experimental focal ischemic brain lesions. With those models, however, a reliable distinction between the ischemic lesions, the border zone, and remote areas of the cortex not directly affected by ischemia is hard to draw because of the variable sizes and shapes of the lesions made.¹ On the other hand, the photothrombosis model by rose bengal and cold light,

a relatively noninvasive model for stroke, has an advantage in that the induced infarcts are highly reproducible in size and location.² Acute small stroke induced by the photo-thrombotic method in rats is homologous to human ischemic cerebral infarcts in histopathology and MRI findings.³

To assess the evolutionary aspects of cerebral ischemic lesions in an experimental stroke model, magnetic resonance imaging (MRI) is currently recommended as a tool.⁴ T2- and/or diffusion-weighted MRI is in fact highly useful for quantitatively predicting histological damage.⁵

Intracerebral neural grafting and cell replacement ther-

Article History:

received 31 May, 2011

accepted 28 July, 2011

Corresponding Author:

Young-Jong Woo
Department of Pediatrics, Chonnam
National University Hospital, 671
Jebong-ro, Dong-gu, Gwangju
501-757, Korea
TEL: +82-62-220-6646
FAX: +82-62-222-6103
E-mail: yjwoo@jnu.ac.kr

apy, which have been used to ameliorate the symptoms of movement disorders such as Parkinson or Huntington disease,⁶ are now proposed as a therapeutic intervention for stroke.⁷⁻⁹ Neural stem cells (NSCs) present in the adult subventricular zone (SVZ) divide themselves slowly and generate a rapidly amplifying progenitor population.¹⁰ It is known that these newly generated neural progenitors migrate from the SVZ to the ischemic striatum after stroke,¹¹ and the process can be confirmed by immunohistochemistry for the phenotypic markers of BrdU.¹²

In this study, we investigated sequential MRI changes correlated with the histological findings of cerebral cortical lesions and the dynamics of endogenous NSCs in an experimental photothrombotic stroke model.

MATERIALS AND METHODS

1. Lesion induction

Male Sprague-Dawley rats (180-330 g) were anesthetized with an intramuscular injection of ketamine (50 mg/kg) and xylazine (5 mg/kg). Body temperature, which was measured by a rectal probe, was maintained constantly at $37.0 \pm 0.5^\circ\text{C}$ by using a heating pad.¹³ Cortical photothrombosis was induced by focusing light to the cortex in rats treated with rose bengal. The skull bone of the rat was fixed on a stereotactic frame, and a cold white light (Olympus, Japan) with a 6 mm aperture was positioned on the skull 1 mm anterior to the bregma and 3 mm lateral to the midline over the right frontal cortex.¹⁴ The photochemical dye rose bengal (20 mg/kg, Sigma, Steinheim, Germany) was infused into the saphenous vein via a microinjection pump, and within 2 minutes the light was applied to the skull for 2 minutes (Fig. 1A).

2. MRI

MRI was performed on a 1.5 T Biospec instrument (Intera®, Philips Medical System, Netherlands). Anesthetized rats were fixed in a stereotactic instrument mounted

in a coil and positioned inside the magnet. The surface coil (Philips Medical System) with an inner diameter of 47 mm was used. T1- and T2-weighted images were obtained at various intervals from 1 hour to 8 weeks after making the lesion (Fig. 1B). Coronal T1-weighted images were obtained. The imaging parameters were TR/TE 500/15 ms, data matrix 224×224, and Fov 50×50 mm. Coronal T2-weighted images were obtained with TR/TE 4108/176 ms, data matrix 128×128, Fov 70×70 mm, and thickness 1 mm. Enhanced images were obtained by means of Gadolinium-DTPA (Magnevist, Scherring, 0.1 mM/kg) injection. To confirm macrophage infiltration to the lesion between 3 and 7 days after stroke, 200 μM -iron/kg superparamagnetic iron oxide (SPIO) was injected, and T2-weighted images (TR/TE 300/13.8 ms, matrix size 224×224, Fov 50×50 mm) were obtained 24 hours after stroke. For further analysis, image data were transferred from the MR console to computers operating JPG image processing software (NIH, Version 1.62, Bethesda, MD, USA).

3. Immunohistochemistry

For immunohistochemistry, all paraffin-embedded sections were cut in 6 μm thicknesses and deparaffinized with xylene and rehydrated in decreasing concentrations of ethanol to water. To re-establish an original conformation of epitopes modified after fixation, the sections were exposed to microwaves in sodium citrate solution. As primary antibodies, monoclonal rat-Nestin IgG (1:100, Chemicon, Temecula, CA), a marker for neural stem and progenitor cells, and monoclonal mouse-Neurofilament protein IgG (NF-L, 1:100, Chemicon, Temecula, CA), a marker for neurons, were used. The tissues incubated with primary antibody were treated with biotinylated secondary antibodies and avidin-biotin complex (ABC, Vector, Burlingame, CA) and were visualized with 3-3' diaminobenzidine tetrahydrochloride (DAB, Chemicon, Temecula, CA) chromogen. The sections were counter-stained with hematoxylin and examined with a light microscope. As controls, sections

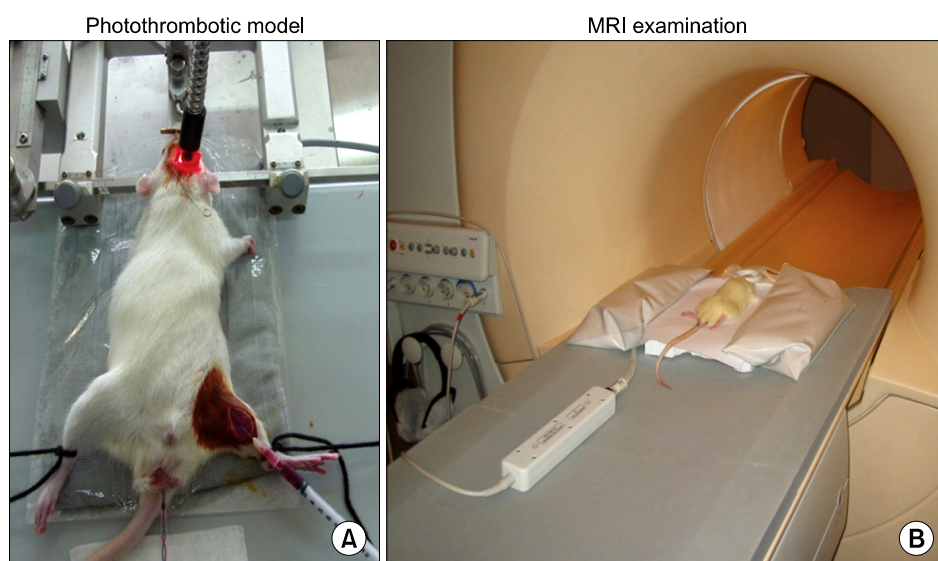


FIG. 1. Photothrombotic model of stroke and MR image. Rosebengal dye (20 mg/kg) was injected via femoral vein and then cold light was applied on the targeted skull overlying motor cortex of rat brain for 20 minutes (A). 1.5 T-MRI with 47 mm diameter surface coil was used for MR images (B).

Serial changes in MRI findings of photothrombotic infarct

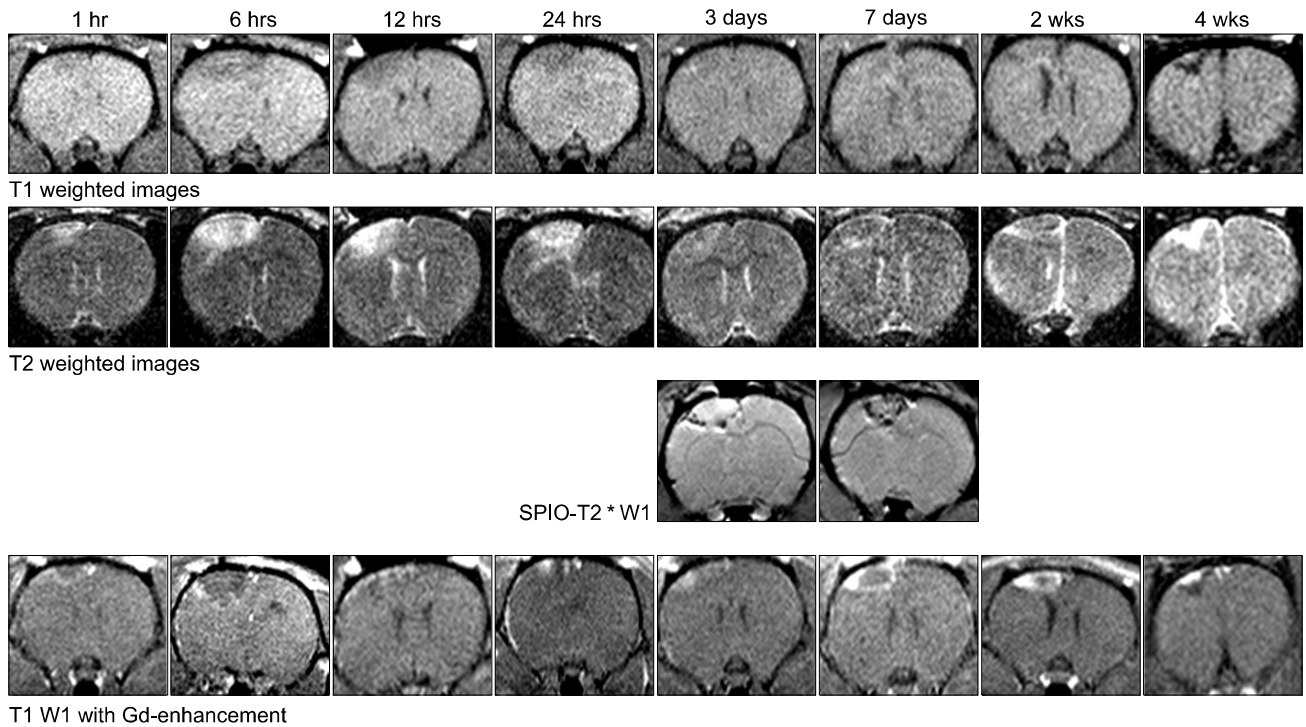


FIG. 2. Early ischemic lesion (6-24 hours) revealed gradually decreased signal intensity of T1 weighted images, while T2 weighted images showed progressive increase of signal intensities. SPIO-T2 images defined macrophages infiltrations around necrosis as dark area between 3-7 days. Gadolinium-enhanced T1 weighted images show the enhancement in the area of fibrosis at 7 days- 4 weeks.

processed with omission of the primary antibody were used.

4. Quantification of endogenous NSC dynamics

Nestin-immunopositive cells were determined in the coronal forebrain sections. The number of NSCs in the SVZ was counted under a microscope. All images were taken at high power (magnification 200×). By use of analysis software, the immunopositive cells in the ischemic boundary region in the cortex, SVZ, and corpus callosum (CC) were counted. For the control, nestin⁺ cells in the SVZ, CC, and similar cerebral cortex of the nonlesional brain were counted. The intracerebral areas indicated the migration tract of the NSCs.

RESULTS

1. MRI

On the T1-weighted images, the signal intensity of the ischemic lesions gradually decreased from 6 to 24 hours. The border zone was blurred in the time intervals. No significant signal changes were noted at 3 to 7 days after stroke. Wedge-shaped decreased signal intensity in the infarct zone was observed at 2 to 4 weeks. On the T2-weighted images, ischemic lesions appeared as high signal intensity areas in the cortex within 24 hours. The high signal intensity was progressively increased up to 12 hours and then slightly reduced. In 3 to 7 days, the signal intensities of the ischemic lesions were gradually decreased nearly to the

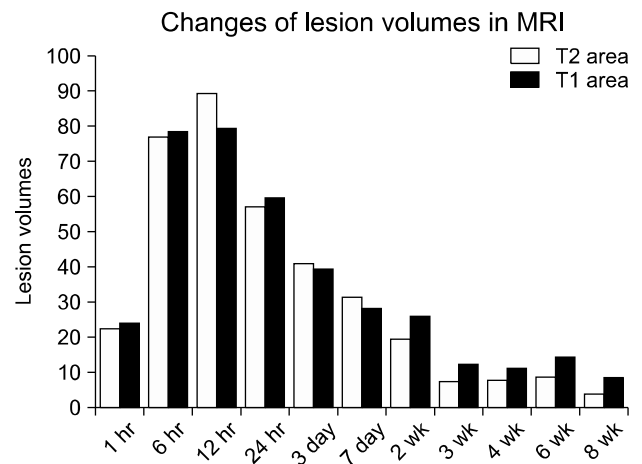


FIG. 3. Changes of infarction volume in MRI. The size of lesion was maximal at 12 hours and then decrease gradually.

level of normal cortex. However, the signal intensities of the deeper margin remained high. In gadolinium-enhanced T1-weighted images, no definitely enhanced lesion was shown at 1 hour to 3 days after stroke. However, there were strong enhancements along the margin of the infarct lesions at 7 days to 4 weeks (Fig. 2). MRI was not enough to explain the cellular changes or massive infiltration of macrophages around the coagulative necrotic lesion. The volume of the lesion was maximal at 12 hours and then de-

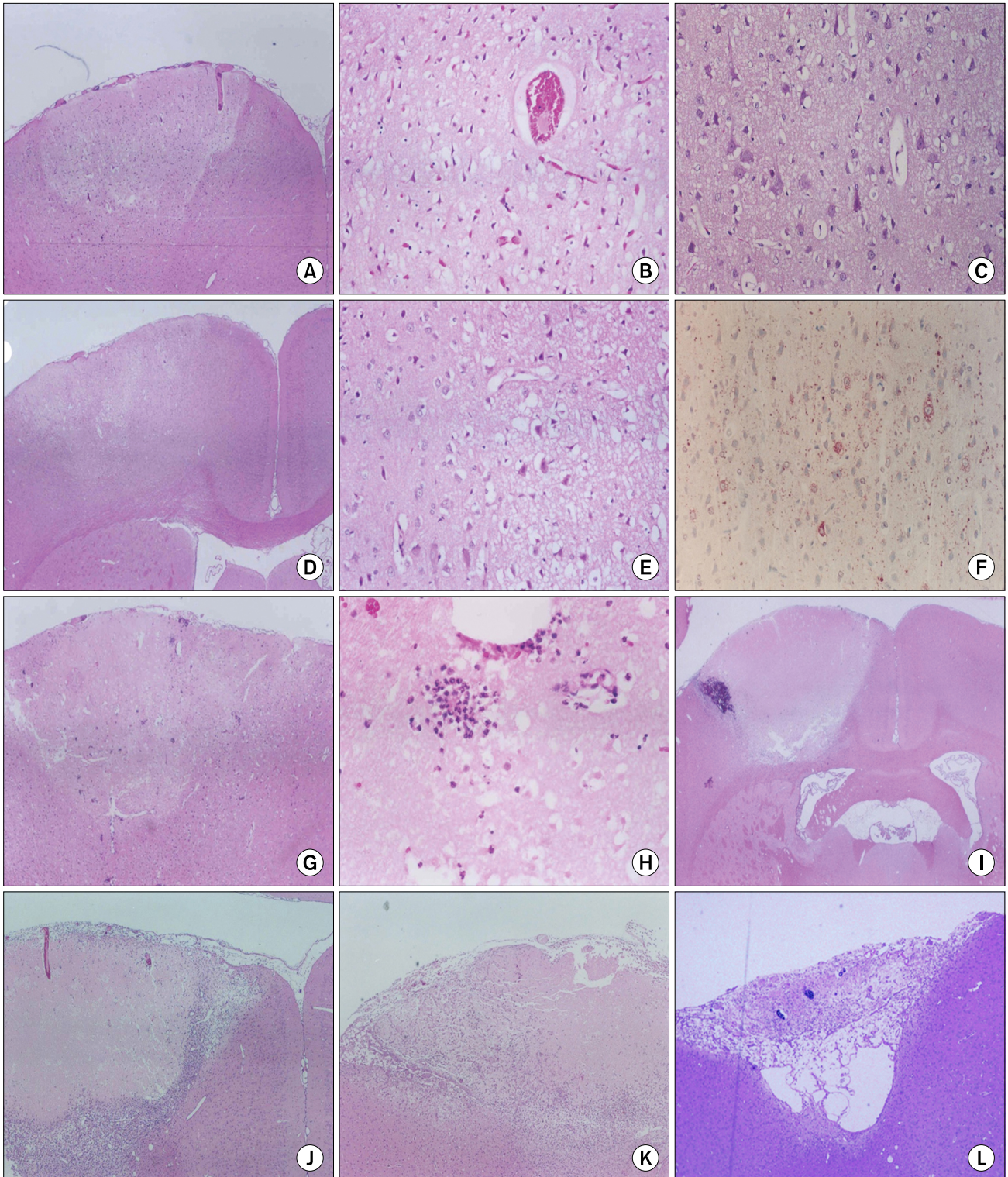


FIG. 4. Histopathology. Half an hour after stroke, wedge shaped edematous lesion consisted of pallor and vacuolation of neuropils at low magnification, high-magnification view revealed dark neurons (A-C). Between 6-12 hours, eosinophilic neurons appeared, which showed swelling of cytoplasm (D, E). The swollen cytoplasm of eosinophilic neurons was positive for NF immunostaining (F). After one day, neutrophil infiltration was shown at the edges of the infarct, and continued to 2 days (G, H). Between 3-7 days, the infarct lesion was characterized by central necrosis surrounded by macrophages and newly formed capillaries (I, J). At 2-4 weeks, cortical necrosis was completely resolved and the lesion was replaced by gliosis and fibrosis (K, L).

creased gradually to 3 weeks (Fig. 3). The area of macrophage infiltration was well demonstrated by the SPIO uptake image, showing linear dark signal intensity at 3 to 7 days.

2. Histopathology

The alterations associated with acute hypoxia-ischemia first became apparent at 30 minutes after ischemia. Half an hour after stroke, a wedge-shaped edematous lesion was seen, showing pallor and vacuolation of neuropils at low magnification. Thrombotic occlusion of superficial capillaries was also frequently noted. The high-magnification view revealed shrinkage of the neuronal cell membrane, cytoplasmic condensation with increased basophilia, and nuclear pyknosis, so-called dark neurons (Fig. 4A-C). After an hour, the boundary of the wedge-shaped lesion developed more pallor. Dark pyknotic neurons were increased in number. Between 6 and 12 hours, eosinophilic neurons appeared, which showed swelling of cytoplasm. Eosinophilic neurons appeared at 6 hours and increased in number between 8 and 12 hours (Fig. 4D, E). The swollen cytoplasm of eosinophilic neurons was positive for NF immunostaining (Fig. 4F). Complete wedge-shaped coagulation necrosis was formed at 24 hours after ischemia. After 1 day, neutrophil infiltration was shown at the edges of the infarct and continued to 2 days (Fig. 4G, H). Between 3 and 7 days, the infarct lesion was gradually reduced and characterized by central necrosis surrounded by macrophages and newly formed capillaries (Fig. 4I, J). At 2 to 4 weeks, cortical necrosis was completely resolved and the lesion was replaced by gliosis and fibrosis. A pseudocavitary lesion was frequently formed (Fig. 4K, L).

3. Correlation of MRI and histopathology

The process of stroke was divided into three stages, and the histopathological findings were compared with the MRI findings in each stage (Table 1). In the acute stage (within 24 hours), histopathology showed a wedge-shaped edematous lesion and red neurons, and corresponding MR

images were low signals on T1-weighted images and high signals on T2-weighted images. In the subacute stage (2-7 days), focal coagulation necrosis and the early reparative process consisting of subsidence of necrosis in the center and transitional area appeared with infiltration of neutrophils and macrophages. The extent and contours of macrophage infiltration were well demonstrated with SPIO as a dark signal area (3-7 days). In the chronic stage (2-8 weeks), the size of the lesion was significantly reduced and the histology revealed gliofibrosis. Gadolinium-enhanced T1-weighted images showed marked enhancement in the areas of fibrosis.

4. Migration of stem cells from the SVZ to the site of injury

The endogenous stem cells in the SVZ on both sides were detected by immunohistochemical stains for nestin. Some nestin⁺ cells emigrated from the SVZ to the CC and cortex, which could be judged by the same morphology of emigrating NSCs. Half an hour after stroke, a few nestin⁺ cells were detected in the SVZ and CC of the lesion side, but no NSCs migrated to the cortex. Stem cells did not migrate to the CC or cerebral cortex of the control side (Fig. 5A). At 12 hours after stroke, nestin⁺ cells were detected in the lesion-side CC and cortex (Fig. 5D-F). At 12 hours, some nestin⁺ cells had migrated to the lesion along the CC. Little migration appeared on the control side, however (Fig. 5G, H). The number of nestin⁺ cells peaked at 2 to 3 days after stroke in both the CC and cortex. A significant number of nestin⁺ cells migrated to the lesion along the CC and were distributed to the peri-lesion area (Fig. 5I-K), and some nestin⁺ cells migrated to the contralateral cortex (Fig. 5L, M). Nestin⁺ cells in the ipsilateral cortex and CC increased at 12 hours to 3 days compared with the contralateral side. In one week, the migration of nestin⁺ cells to the lesion-side CC and the boundary of the cortex decreased significantly. The emigration of endogenous NSCs from the SVZ to the CC and cortex changed with time (Table 2, Fig. 6). The number of nestin⁺ cells in the contralateral SVZ was similar to that in the ipsilateral SVZ in each group. Nestin⁺ cells ap-

TABLE 1. MRI and histopathologic findings in photothrombotic infarction

Stage of infarct (Time)	MR sequence	Characteristic finding	Histopathology
Acute stage (<24 hours)	T1WI	Low SI	Wedge-shaped edema and red neurons
	T2WI	High SI	
Subacute stage (2-7 days)	T1WI	Center: SI ↓ Periphery: SI ↑	Center: subsidence of edema Periphery: transitional area
	T2WI	Center: SI ↑ Periphery: SI ↓	
	Gd -T1WI SPIO image	Parenchymal enhancement Wedge shaped low density	Macrophage infiltration
Chronic stage (2-8 weeks)	T2WI	Center: iso-SI Periphery: SI ↓ (<4 weeks) SI increased by addition of cystic change (>4 weeks)	Gliofibrosis (<4 weeks) Gliofibrosis and cystic change (>4 weeks)
	Gd -T1WI	Marked enhancement (<4 weeks) Enhancement maintained (>4 weeks)	

T1WI: T1 weighted images, T2WI: T2 weighted images, Gd-T1WI: gadolinium-enhanced T1 weighted images, SI: signal intensity.

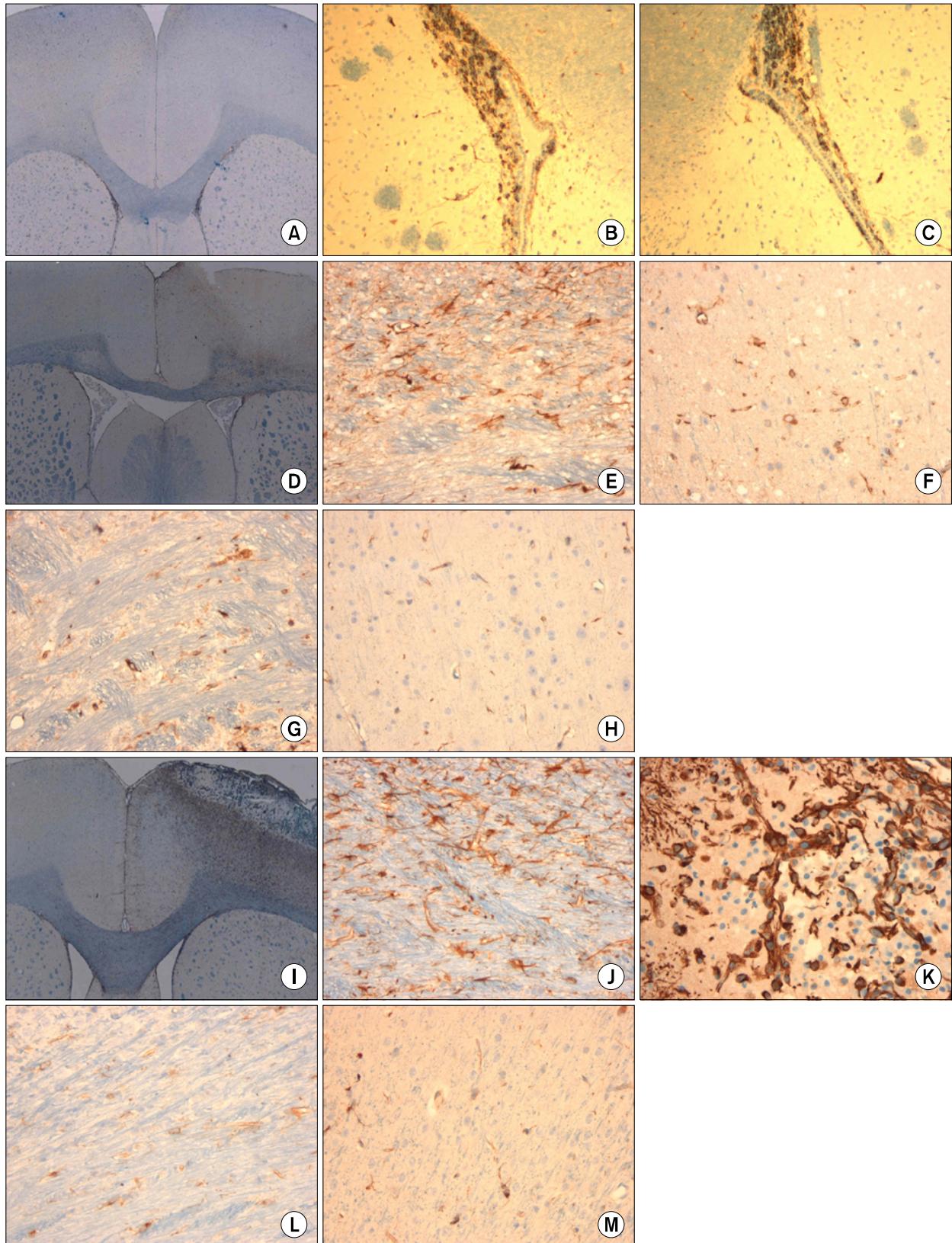


FIG. 5. Migration of neural stem cells (NSCs) from the subventricular zone (SVZ) to the cortical infarct lesion. There is no difference of Nestin⁺ NSCs in the SVZ at 0.5 hour after ischemia (A-C). Significantly increased number of Nestin⁺ NSCs along the corpus callosum (CC) and cerebral cortex at 12 hours after ischemia (D-H). Markedly increased number of Nestin⁺ NSCs in the white matter of cerebral cortex and the infarct lesion at 3 days after ischemia (I-M). (A, D, I; H&E stain, B, E, F, J, K; nestin, ischemic side, C, G, H, L, M; nestin, non-ischemic side).

TABLE 2. Quantitative number of nestin⁺ NSCs in the subventricular zone (SVZ), corpus callosum (CC), and cerebral cortex (C)

Time after stroke	Lesion side			Control side		
	SVZ	CC	C	SVZ	CC	C
0.5 hour	50.5	0.4	0	47.5	0	0
1 hour	31.5	0	0	31	0	0
2 hours	57.5	0	0	22	0	0
4 hours	44	5	1	48	0.5	0
6 hours	31.5	2.5	0	29.5	0	0
12 hours	36.5	2	2	38.5	1	0.5
24 hours	23.5	13	7	28.5	2.5	2.5
2 days	20.5	20.5	12.5	20	4	6.5
3 days	22	19.5	20.5	17	2.5	0.5
1 week	45	7.6	13.5	44.3	0.4	0
2 weeks	22.3	4.3	6.3	15.3	0	0

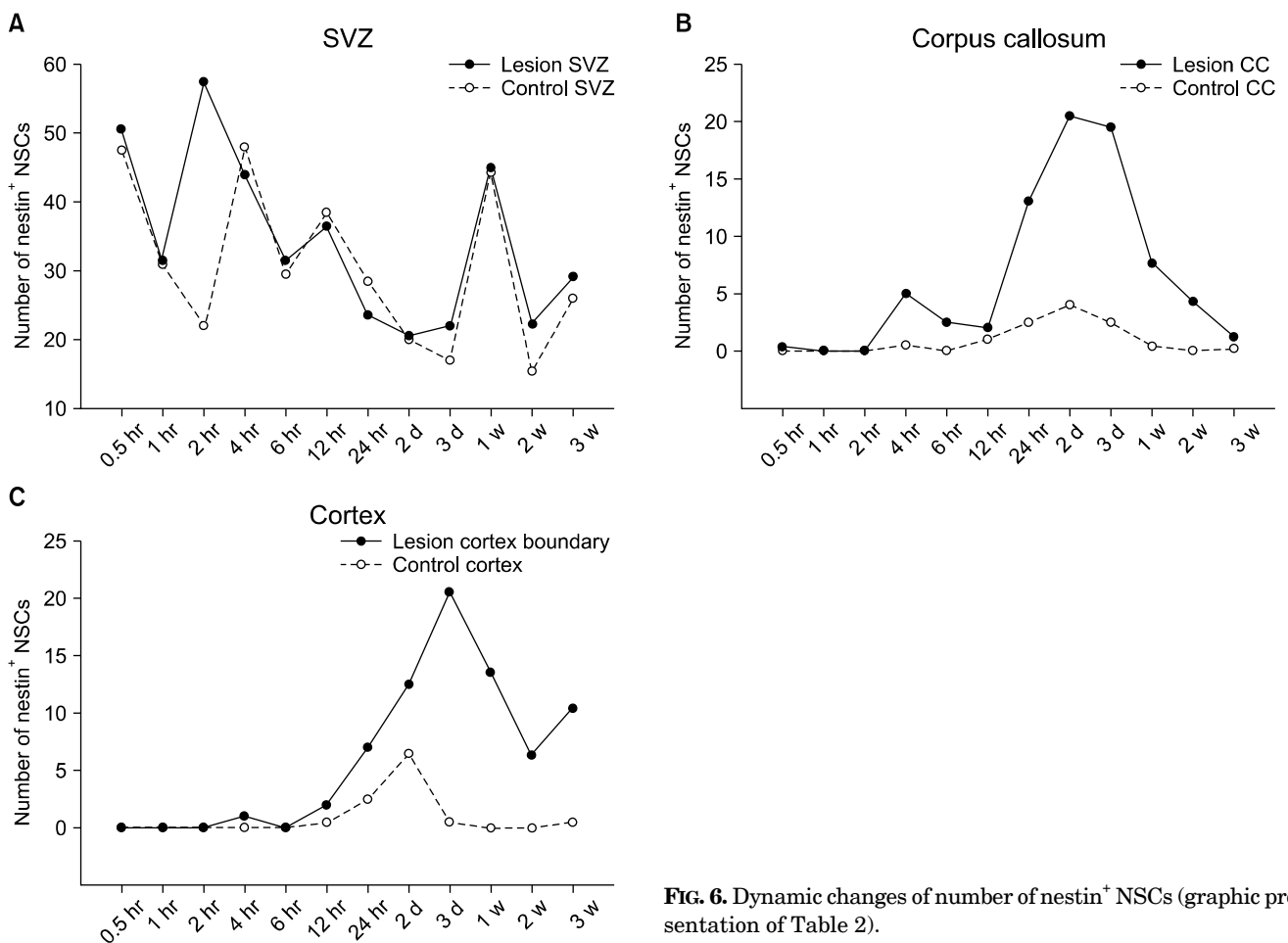


FIG. 6. Dynamic changes of number of nestin⁺ NSCs (graphic presentation of Table 2).

peared as chains oriented toward the ischemic boundary lesions, formed clusters, and dispersed in the ipsilateral cortex (Fig. 5K).

DISCUSSION

1. Stroke: acute damage

Stroke is an acute, progressive event. More than one-fourth of neurons become swollen and chromatolytic with

vacuoles during the 3 days after a 2-hour occlusion of the MCA.¹⁵ Cellular alterations are evident at 4 hours after occlusion, i.e., the cell death is acute, without an initial latent period as in the delayed neuronal death noticed in the hippocampus.¹⁶ In this experiment, the infarct lesion even appeared within 30 minutes after induction of ischemia. The ischemic lesion of the photothrombotic model developed rapidly with time during the early stage.

MR imaging has become a powerful tool for accurate and

fast assessment of early ischemic damage in animal models and clinical investigations of stroke.¹⁷ In this study, the volume of the lesion was maximal at 12 hours in T2-weighted images and then decreased rapidly. A small, cortical hyperintense area was noticeable within 15 to 20 minutes after photochemical induction of stroke and expanded within the next 4 hours on both diffusion- and T2-weighted images. The DWI hyperintensity was maximal at 3 to 10 hours after photothrombosis.¹⁸

2. Early ischemic infarction in the rat brain with MRI and histological correlation

T2-weighted images are very helpful to see the evolution of the infarct lesion over 24 hours due to the progressive increase in signal intensities. In histology, within 24 hours, the lesions appeared as wedge-shaped, pale edematous lesions in the gray matter that became paler as time progressed. Complete necrosis presented at 24 hours. Histology corresponded with MRI in an early stroke model, and the increased signals of the T2-weighted images corresponded with cellular changes of edema and infarction within 24 hours in this study. One hour after infarction, the lesion became well defined and hyperintense on the T2-weighted images, and these changes were more exaggerated between 6 and 12 hours and then decreased from 24 hours after stroke. Photomicrographs of histologic sections stained with H&E showed the most striking features—swelling of the neuropil and pronounced swelling of the perineural astroglial processes—in which the center of the lesion had no intact cells at 24 hours. Between 3 and 7 days after ischemia, the lesion was reduced in intensity, with an intensity similar to healthy cortex on T2-weighted images, especially with SPIO injection.

Studies performed in patients with acute stroke have also proved that diffusion-weighted MR imaging is useful for the early identification of ischemic regions.¹⁹ The advantage of this stroke model is that it is easily reproduced, is noninvasive, and MR images can be obtained with time in the same rat. Dietrich et al found that the water content within the irradiated zone is significantly elevated 15 minutes after exposure to light on T2-weighted images.²⁰ The lesions could be detectable even within half an hour of induction of the ischemia because of the characteristics of the photothrombotic lesion.

Another report showed that the MRIs of the infarcts revealed a discrete zone of abnormal cortical signal, with a mean depth of 2.31 mm, close to the measured mean depth of the necrotic zones in the cortex in the histological sections of 2.5 mm. MRI also showed a bordering transitional zone of T2 hyperintensity of 2.0 mm, which was close to the 1.7 mm mean thickness of the vacuolated zone bordering the infarcts histologically. There was not only a qualitative correlation but also a close quantitative correlation of the MR infarct images to the histologic infarct patterns.⁵ In the present study, the volume of the lesion was maximal at 12 hours and then decreased gradually to 3 weeks, which corresponded quantitatively to the histological changes.

Histological patterns were also identical to that finding. Within the infarct zone, cortical neurons were all hyper-eosinophilic with pyknotic and shrunken nuclei, which was a similar morphology to the transition zones. Abnormal neurons gradually gave way to normal neurons in the vacuolated zones. MRIs of these infarcts in vivo closely corresponded to the histologic appearance of the lesions.

3. Stem cells migrate from the SVZ to the boundary of the ischemic infarct

A number of stem cells significantly increased in the SVZ and migrated to the ischemic boundary, especially between 2 and 3 days after stroke. In adult brain, doublecortin is primarily expressed in migrating and differentiating neurons in the SVZ and rostral migratory stream.²¹ Observation of a significant increase in doublecortin-positive cells in the ipsilateral striatum suggests that these cells may migrate from the SVZ. Electronic microscopy revealed that the cluster cells in the ipsilateral striatum had spindle-shaped dark nuclei, many free ribosomes in the cytoplasm, open extracellular spaces, and tight junctions. Ultrastructural data demonstrate that cells in the ipsilateral striatum have morphologic characteristics of cells in the SVZ.²² In stem cell transplantation, the injection tract mainly along the CC and the stem cell were attracted by the lesion site. Preferential migration of stem cells toward the site of a lesion is a highly desirable property of stem cells that allows flexibility in the site of graft implantation in the damaged brain.²³ Neural stem cells migrated from the SVZ mainly along the CC and migrated to the boundary, especially at the 2 to 3 day time point. Thus, our findings agree that endogenous NSCs migrated from the SVZ to the ischemic boundary.

In conclusion, in this photothrombotic stroke model, MRIs of the lesional cortex correlated well with histopathologic findings, which could be divided into three stages: acute (edema and necrosis) within 24 hours, subacute (acute and chronic inflammatory cell infiltration) at 2 to 7 days, and chronic (gliofibrosis) at 2 to 8 weeks. The volume of the infarct was significantly reduced by reparative gliofibrosis. Active emigration of internal NSCs from the SVZ toward the infarct lesion may also contribute to repairing the infarct lesion, but the self-repair mechanism by endogenous NSCs is insufficient to treat stroke causing extensive neuronal death. Further studies should be focused on amplification technologies of NSCs emigrating from the SVZ to enhance the collection of endogenous or transplanted NSCs for the treatment of stroke.

ACKNOWLEDGEMENTS

This study was financially supported by Chonnam National University, 2005.

Lee MC and Jin CY were equally contributed to the study.

REFERENCES

1. Nedergaard M. Neuronal injury in the infarct border: a neuropathological study in the rat. *Acta Neuropathol* 1987;73:267-74.
2. Watson BD, Dietrich WD, Busto R, Wachtel MS, Ginsberg MD. Induction of reproducible brain infarction by photochemically initiated thrombosis. *Ann Neurol* 1985;17:497-504.
3. Pevsner PH, Eichenbaum JW, Miller DC, Pivawer G, Eichenbaum KD, Stern A, et al. A photothrombotic model of small early ischemic infarcts in the rat brain with histologic and MRI correlation. *J Pharmacol Toxicol Methods* 2001;45:227-33.
4. Hossmann KA, Hoehn-Berlage M. Diffusion and perfusion MR imaging of cerebral ischemia. *Cerebrovasc Brain Metab Rev* 1995;7:187-217.
5. Loubinoux I, Volk A, Borredon J, Guirimand S, Tiffon B, Seylaz J, et al. The effects of a butanediol treatment on acute focal cerebral ischemia assessed by quantitative diffusion and T2 MR imaging. *Magn Reson Imaging* 1997;15:1045-55.
6. Björklund A, Lindvall O. Cell replacement therapies for central nervous system disorders. *Nat Neurosci* 2000;3:537-44.
7. Borlongan CV, Tajima Y, Trojanowski JQ, Lee VM, Sanberg PR. Cerebral ischemia and CNS transplantation: differential effects of grafted fetal rat striatal cells and human neurons derived from a clonal cell line. *Neuroreport* 1998;9:3703-9.
8. Kondziolka D, Wechsler L, Goldstein S, Meltzer C, Thulborn KR, Gebel J, et al. Transplantation of cultured human neuronal cells for patients with stroke. *Neurology* 2000;55:565-9.
9. Nishino H, Borlongan CV. Restoration of function by neural transplantation in the ischemic brain. *Prog Brain Res* 2000;127:461-76.
10. Romanko MJ, Rola R, Fike JR, Szele FG, Dizon ML, Felling RJ, et al. Roles of the mammalian subventricular zone in cell replacement after brain injury. *Prog Neurobiol* 2004;74:77-99.
11. Zhang R, Zhang Z, Wang L, Wang Y, Gousev A, Zhang L, et al. Activated neural stem cells contribute to stroke-induced neurogenesis and neuroblast migration toward the infarct boundary in adult rats. *J Cereb Blood Flow Metab* 2004;24:441-8.
12. Sundholm-Peters NL, Yang HK, Goings GE, Walker AS, Szele FG. Subventricular zone neuroblasts emigrate toward cortical lesions. *J Neuropathol Exp Neurol* 2005;64:1089-100.
13. Arai K, Igarashi H, Arai T, Katayama Y. The effect of ozagrel sodium on photochemical thrombosis in rat: therapeutic window and combined therapy with heparin sodium. *Life Sci* 2002;71:2983-94.
14. Paxinos G, Watson CR, Emson PC. AChE-stained horizontal sections of the rat brain in stereotaxic coordinates. *J Neurosci Methods* 1980;3:129-49.
15. Yamada K, Goto S, Sato K, Yoshikama M, Okamura A, Nagahiro S, et al. 'Reactive change' of the sub-stantia nigra neurons subsequent to striatal infarction in rats. *Biomed Res* 1996;17:339-46.
16. Kirino T, Sano K. Fine structural nature of delayed neuronal death following ischemia in the gerbil hippocampus. *Acta Neuropathol* 1984;62:209-18.
17. Rordorf G, Koroshetz WJ, Copen WA, Cramer SC, Schaefer PW, Budzik RF Jr, et al. Regional ischemia and ischemic injury in patients with acute middle cerebral artery stroke as defined by early diffusion-weighted and perfusion-weighted MRI. *Stroke* 1998;29:939-43.
18. Pierpaoli C, Righini A, Linfante I, Tao-Cheng JH, Alger JR, Di Chiro G. Histopathologic correlates of abnormal water diffusion in cerebral ischemia: diffusion-weighted MR imaging and light and electron microscopic study. *Radiology* 1993;189:439-48.
19. Warach S, Chien D, Li W, Ronthal M, Edelman RR. Fast magnetic resonance diffusion-weighted imaging of acute human stroke. *Neurology* 1992;42:1717-23.
20. Dietrich WD, Busto R, Watson BD, Scheinberg P, Ginsberg MD. Photochemically induced cerebral infarction. II. Edema and blood-brain barrier disruption. *Acta Neuropathol* 1987;72:326-34.
21. Komitova M, Mattsson B, Johansson BB, Eriksson PS. Enriched environment increases neural stem/progenitor cell proliferation and neurogenesis in the subventricular zone of stroke-lesioned adult rats. *Stroke* 2005;36:1278-82.
22. Doetsch F, García-Verdugo JM, Alvarez-Buylla A. Cellular composition and three-dimensional organization of the subventricular germinal zone in the adult mammalian brain. *J Neurosci* 1997;17:5046-61.
23. Modo M, Mellodew K, Cash D, Fraser SE, Meade TJ, Price J, et al. Mapping transplanted stem cell migration after a stroke: a serial, in vivo magnetic resonance imaging study. *Neuroimage* 2004;21:311-7.